Systematic Errors in Global Radiosonde Precipitable Water Data from Comparisons with Ground-Based GPS Measurements

JUNHONG WANG AND LIANGYING ZHANG

Earth Observing Laboratory, National Center for Atmospheric Research, Boulder, Colorado*

(Manuscript received 8 March 2007, in final form 19 September 2007)

ABSTRACT

A global, 10-yr (February 1997–April 2006), 2-hourly dataset of atmospheric precipitable water (PW) was produced from ground-based global positioning system (GPS) measurements of zenith tropospheric delay (ZTD) at approximately 350 International Global Navigation Satellite Systems (GNSS) Service (IGS) ground stations. A total of 130 pairs of radiosonde and GPS stations are found within a 50-km distance and 100-m elevation of each other. At these stations, 14 types of radiosondes are launched and the following 3 types of humidity sensors are used: capacitive polymer, carbon hygristor, and goldbeater's skin. The PW comparison between radiosonde and GPS data reveals three types of systematic errors in the global radiosonde PW data: measurement biases of the 14 radiosonde types along with their characteristics, long-term temporal inhomogeneity, and diurnal sampling errors of once- and twice-daily radiosonde data. The capacitive polymer generally shows mean dry bias of −1.19 mm (−6.8%). However, the carbon hygristor and goldbeater's skin hygrometers have mean moist biases of 1.01 mm (3.4%) and 0.76 mm (5.4%), respectively. The protective shield over the humidity sensor boom introduced in late 2000 reduces the PW dry bias from 6.1% and 2.6% in 2000 to 3.9% and −1.14% (wet bias) in 2001 for the Vaisala RS80A and RS80H, respectively. The dry bias in Vaisala radiosondes has larger magnitudes during the day than at night, especially for RS90 and RS92, with a day–night difference of 5%–7%. The time series of monthly mean PW differences between the radiosonde and GPS are able to detect significant changes associated with known radiosonde type changes. Such changes would have a significant impact on the long-term trend estimate. Diurnal sampling errors of twice-daily radiosonde data are generally within 2%, but can be as much as 10%–15% for the once-daily soundings. In conclusion, this study demonstrates that the global GPS PW data are useful for identifying and quantifying several kinds of systematic errors in global radiosonde PW data. Several recommendations are made for future needs of global radiosonde and GPS networks and data.

1. Introduction

Global radiosonde data still represent an important resource for initializing numeric weather models, monitoring and understanding climate changes, conducting global and regional reanalyses, and calibrating and validating satellite data. In recent years, radiosonde data have received increased attention in climate research because the data provide the longest record (the last six decades) of upper-air temperature, humidity, and wind; have near-global coverage; and have high vertical resolution. However, the role of radiosonde data in the climate study is limited, in part, by sensor characteristics that vary substantially in time and space. This study focuses on the radiosonde humidity errors.

Global radiosonde climatic records suffer from three types of errors: systematic observational error, spatial and temporal inhomogeneity, and diurnal and spatial sampling errors. For humidity, systematic observational errors can be attributed to specific sensor limitations, such as contamination, miscalibration, time lag, or hysteresis. They can also be due to external factors, such as problems in data reporting practices or faulty ground checks. Most previous studies have been focused on Vaisala and Sippican (formally VIZ) radiosondes. The contamination dry bias in the Vaisala radiosonde data along with other errors have been found and corrected in various studies (e.g., Soden and Lanzante 1996; Zipser and Johnson 1998; Wang et al. 2002a; Turner et al. 2003; Soden et al. 2004; Nakamura et al. 2004). Sev-

* The National Center for Atmospheric Research is sponsored by the National Science Foundation.

Corresponding author address: Junhong Wang, NCAR/EOL, P.O. Box 3000, Boulder, CO 80307.
E-mail: junhong@ucar.edu

DOI: 10.1175/2007JCLI1944.1

eral shortcomings of the VIZ carbon hygristor humidity sensor have also been found (e.g., Wade 1994; Elliott et al. 1998; Wang et al. 2003; Wang and Young 2005). The World Meteorological Organization (WMO) radiosonde intercomparison projects also provide insights on the performance of operational radiosondes (Nash et al. 2005). The changes in humidity sensors at a given station introduce a discontinuity in the long-term water vapor records (cf. Angell et al. 1984; Elliott and Gaffen 1991; Elliott et al. 1998; Ross and Gaffen 1998; Soden and Schroeder 2000; Wang et al. 2001; Elliott et al. 2002). All the past efforts primarily focused on humidity sensors of Vaisala and VIZ radiosondes. There is little known about the humidity errors of the other 9 types out of the total 14 types used in the current global radiosonde network, and their resulting impact on the long-term climate record. Because of the mixture of 14 radiosonde types and their distinct error characteristics, global radiosonde data carry the spatial inhomogeneity error. Diurnal sampling errors of once- or twice-daily radiosonde data are hard to quantify because of a lack of data with enough diurnal samples. However, substantial diurnal variations in atmospheric water vapor, both column-integrated values [i.e., precipitable water (PW)] and vertical profiles (e.g., Dai et al. 2002; Wang et al. 2002b), have been found and could induce nonnegligible sampling errors if observations are made only a few times a day.

One important task in obtaining a homogeneous radiosonde climate record involves developing global metadata and statistical approaches to identify, record, and consequently correct known observational changes and errors (e.g., Gaffen 1993; Zurbenko et al. 1996). Several methods developed to correct humidity observational errors in individual types of radiosondes include laboratory or physically based correction schemes (e.g., Crutcher and Eskridge 1993; Leiterer et al. 1997; Wang et al. 2002a; Ciesielski et al. 2003), statistical approaches using comparisons with other data (e.g., Lucas and Zipser 2000; Miloshevich et al. 2001; Sharpe and Macpherson 2001; Vömel et al. 2007), and a scaling method using independent, coincident PW data (Turner et al. 2003). All these correction methods were developed for Vaisala and VIZ radiosondes in specific temporal and spatial domains, and so have limited applications to the global humidity dataset. There is very little knowledge on the performance of Russian MRZ/Mars, Chinese Shang, and Indian IM-MK3 radiosondes although they are launched at 29% of the global radiosonde stations. In addition, without an independent reference instrument or dataset, these approaches cannot be validated and necessarily retain a degree of uncertainty that limits their widespread application.

The global positioning system (GPS) consists of 30 satellites in six orbit planes transmitting L-band radio signals to ground-based GPS receivers around the globe. The radio signals are delayed by the atmosphere when traveling from the satellite to the ground, referred as total delay. Atmospheric integrated water vapor (i.e., PW) can be obtained from the GPS signal delay (Bevis et al. 1992, 1994; Rocken et al. 1993, 1997). The International Global Navigation Satellite Systems (GNSS) Service (IGS) network includes more than 350 ground-based GPS stations around the globe. A global, 2-hourly PW dataset has been produced using the IGS zenith tropospheric delay (ZTD) products (Wang et al. 2007). The advantages of GPS-derived PW include data available under all weather conditions, high temporal resolution (5 min to 2 hourly), high accuracy ($<$3 mm in PW), and long-term stability. All of these advantages make the GPS-derived PW data very appealing to identify and quantify the three types of errors in the long-term radiosonde PW data described above.

Radiosonde humidity data are often used to estimate the accuracy of GPS-derived PW (e.g., Tregoning et al. 1998; Ohtani and Naito 2000; Dai et al. 2002; Bokoye et al. 2003; Guerova et al. 2003; Li et al. 2003; Nakamura et al. 2004; Deblonde et al. 2005). However, the PW discrepancies between radiosonde and GPS data found in these studies are often a result of errors in the radiosonde data. Most of these comparisons have only been done on short time scales from several weeks to several years and at several stations, and only briefly mention systematic errors in radiosonde data. The study of Dai et al. (2002) is the only one to quantify the diurnal sampling errors of twice-daily radiosonde data, but it is only for the United States. There have been no studies to take advantage of the long-term stability of the GPS data to identify the discontinuity of radiosonde humidity records.

The goal of this study is to use a near-global, 2-hourly, 10-yr (1997–2006) PW dataset constructed from ground-based GPS measurements to identify and quantify systematic errors in the global radiosonde PW data. Three kinds of systematic errors are studied: measurement biases and their characteristics for 14 types of radiosondes used in the global radiosonde network, long-term temporal inhomogeneity, and diurnal sampling errors of once- and twice-daily radiosonde data. Section 2 describes the details about the radiosonde, GPS, and matched radiosonde–GPS datasets, and discusses factors contributing to the PW differences between the radiosonde and the GPS data. Section 3 presents comparison results on three kinds of systematic errors in global radiosonde PW data. Section 4 summa-

rizes main results and makes some recommendations on future needs of radiosonde and GPS data.

2. Data

a. Global GPS PW and radiosonde datasets

A global, 2-hourly PW dataset was produced from the ZTD derived from ground-based GPS measurements at between 80 and 268 IGS stations (see Figs. 1 and 2 in Wang et al. 2007), increasing in time. The ZTD data are available online (see ftp://cddis.gsfc.nasa.gov/gps/products/trop/). The GPS-derived PW is found to exhibit no systematic errors and has a RMS error of less than 3 mm based on comparisons with radiosonde, microwave radiometer (MWR), and satellite data (Wang et al. 2007). The dataset also contains other supplemental data, including 2-hourly surface pressure, water vapor weighted mean temperature of the atmosphere (Tm), ZTD, and zenith hydrostatic and wet delay. This dataset will be continuously updated as soon as the ZTD and other auxiliary data become available.

The Integrated Global Radiosonde Archive (IGRA) produced by the National Climatic Data Center (NCDC) is used in this study and is compiled from 11 datasets (Durre et al. 2006). A series of rigorous quality assurance procedures have been applied to these component datasets to create a larger and more comprehensive dataset. IGRA consists of 1–4 radiosonde observations per day at more than 1500 globally distributed stations from 1938 to the present. The dataset includes pressure, temperature, geopotential height, dewpoint depression, wind direction, and wind speed at standard, surface, tropopause, and significant levels. The IGRA dataset can be obtained from the NCDC FTP Web site (online at ftp://ftp.ncdc.noaa.gov/pub/data/igra).

The PW is calculated from the IGRA data by integrating specific humidity from the surface to the top of the sounding profile. The dewpoint depression (ΔT_d) is given in the IGRA data and is converted to specific humidity by using the following Eq. (1) [Eq. (10) in Bolton 1980] for the vapor pressure calculation and Eq. (2):

$$e = 6.112 \exp\left(\frac{17.67 T_d}{T_d + 243.5}\right), \tag{1}$$

$$q = \frac{\epsilon e}{P - (1 - \epsilon)e}, \tag{2}$$

where e is vapor pressure (hPa), T_d is dewpoint temperature (°C) and equals to $T - \Delta T_d$ (T is temperature in °C), q is specific humidity (kg kg^{-1}), and $\epsilon = 0.622$.

An analysis was conducted on how sensitive the PW is to no data above the tropopause, 300, 500, and 700 hPa; also on missing data at the surface, 1000, and 850 hPa using global and annual mean profiles of temperature and humidity calculated from the IGRA data. The sensitivity analysis shows that the PW is sensitive to missing data at the surface, 1000, and 850 hPa; no data above 300 hPa would only introduce a dry bias of 0.61% in the PW. Therefore, for the PW calculation we required radiosonde temperature and humidity profiles to reach at least 300 hPa and have data available at the surface and at least five (four) standard pressure levels above the surface for stations below (above) 1000 hPa. As shown in Figs. 7 and 8 in Durre et al. (2006), the vertical resolution and extent of the soundings have improved significantly over the years. By 2003, the average sounding contains 11 mandatory and 35 additional levels, and 74% of all soundings reach at least 100 hPa.

b. Matched radiosonde and GPS PW data

Global radiosonde and GPS PW data from February 1997 to April 2006 are first matched in space (both horizontally and vertically). There are a total of 130 matched pairs of stations where GPS and radiosonde stations are located within 50 km and have elevation differences less than 100 m. The geographic distribution of matched stations is displayed in Fig. 1. During the study period, 14 types of radiosondes are used at these stations and are shown by different colors in Fig. 1. The detailed information on the radiosonde types is given in Table 1. RS80A, RS80H, RS90, and RS92 all belong to the Vaisala radiosonde series, in which RS80A is the oldest one and RS92 is the newest one. Note that the radiosonde type might have been changed from 1997 to 2006 at a given station. For such a case, more than one type of radiosonde is shown at the station in Fig. 1 with a slight shift in the station location, and more than one matched pair of stations is counted according to radiosonde types. As a result, the total matched pairs of stations are 169 for comparison of the 14 types of radiosondes. As of February 2006, there are 14 types of radiosondes launched in the global radiosonde network (WMO 2006). Among them, only one type, the Swiss radiosonde (ML-SRS), is not studied here (Table 1). After matched stations are identified, the GPS PW data within an hour of the radiosonde launch time are selected for comparison. At least 100 pairs of matched data points are required for each matched station.

There is no information on radiosonde types in the IGRA data. We first obtain the radiosonde type information from the WMO report, "WMO Catalogue of Radiosondes and Upper-air wind Systems" updated in 2001 and on 10 January 2002, 30 October 2004, and 1

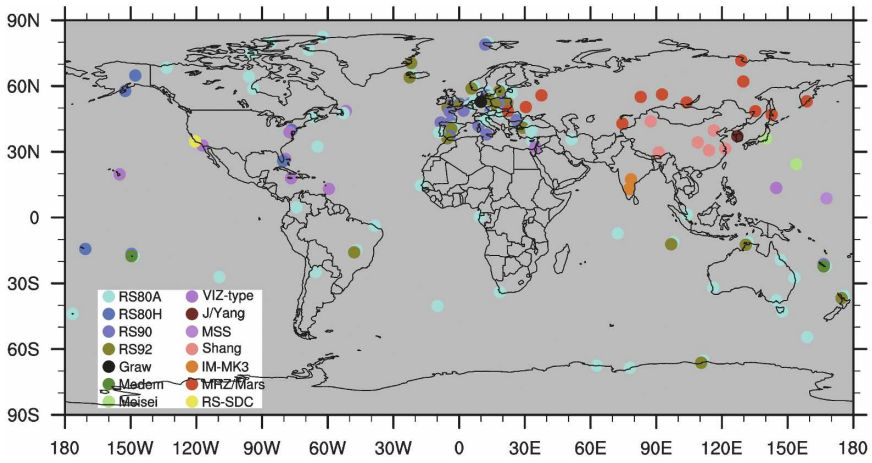

FIG. 1. Geographic distributions of matched radiosonde and GPS stations. Different colors denote the 14 radiosonde types. When the radiosonde type change has taken place during the period, the station locations are moved a little bit to show the second and/or third types.

February 2006 (WMO 2006). The 2001 version includes updates from November 1996 to December 2001. If two consecutive versions show different radiosonde types, the date for such change is assumed to be the date of the later version of the WMO Catalogue, although the change could have occurred any time between the dates of two versions. Then several other resources on the radiosonde types are checked, including Elliott et al. (1998) and H. Facundo and W. Blackmore (2006, personal communications) for the U.S. radiosonde network; Gaffen (1993) and subsequent periodical updates for the global network; IGRA metadata (available online at http://www.ncdc.noaa.gov/oa/cab/igra/index.php?name=metadata); and R. Atkinson and S. Allen (2006, personal communications) for the Australian stations. Finally the time series of PW differences (IGRA minus GPS) are visually examined to look for any large and apparent jumps that do not correspond to identified radiosonde type changes and any known changes affecting the GPS PW data. The determination on the jumps is subjective. If the dates for these jumps occurred between two WMO updates, they are assumed to be correct dates of radiosonde type changes. The stations where such corrections are applied are summarized in Table 2. Table 3 lists all stations with radiosonde type changes and the starting and ending dates of the radiosonde types used at these stations. A total of 33 stations experienced the type changes during 1997–2006; most of them consisted of two types.

After the procedure described above is implemented, a matched radiosonde and GPS PW database is produced. The comparisons presented in section 3 are made based on radiosonde types. The total number of matched stations and data points is presented in Fig. 2 for each radiosonde type. Vaisala RS80A is used in 66 matched stations, while only one matched station is found for each of Graw, RS-SDC, J/Yang, and MSS radiosondes. There are a total of 115 034 matched data points for RS80A comparison, but less than 300 for RS-SDC and Modem.

c. *Factors contributing to PW differences*

Several factors can contribute to the PW differences at matched stations: differences in measurement techniques, the errors of radiosonde and GPS data, and separations of radiosonde and GPS stations. Since this study is focusing on identifying systematic errors in radiosonde data, efforts have been made to minimize the contributions of all these factors except the radiosonde's systematic errors to the PW differences presented in section 3.

As illustrated in Fig. 11 of Liou et al. (2001), ground-based GPS receivers and radiosondes sample different volumes of the atmosphere. GPS measures the atmosphere along the path from the receiver to the satellite; the delay along the path is mapped onto the zenith direction by assuming a stratified atmosphere. At stations with very high elevations, the assumption of atmospheric isotropy in the boundary layer often does not hold, resulting in errors in the GPS-estimated PW (Hagemann et al. 2003). Radiosondes drift horizontally on an order of 20 km from the surface to 10 km, so they measure the atmosphere along the radiosonde trajectory. The PW difference due to this horizontal drift is difficult to assess since it is subject to the degree of atmospheric inhomogeneity. However, the error contributing to the differences in measurement techniques is most likely to be random for the majority of cases, so

TABLE 1. Radiosonde main types and subtypes, manufacturers, their humidity sensors, number and percentage of stations using each main type in current global radiosonde network, and number of stations for each main type in our matched database for all times.

Type	Manufacturer	Subtypes	Humidity sensor	No. of stations	Percentage of stations	Matched No. stations
RS80A	Vaisala (Finland)	VRS80, VRS80G, RS80G, GPS-RS80–15G, VRS80–15G, VRS80L, VRS80N	A-Humicap	229	26.97	66
RS80H	Vaisala (Finland)	VRS80–57H, VRS80H, VRS80LH, VRS80GH	H-Humicap	68	8.01	12
RS90	Vaisala (Finland)	RS90G, VRS90, VRS90AL, VRS90G, VRS90G/L, VRS90L	Twin Humicaps	37	4.36	22
RS92	Vaisala (Finland)	VRS92, VRS92-AGP, VRS92G/L, VRS92LH, VRS92G, VRS92L, VRS92KL	Twin Humicaps	130	15.31	23
RS-SDC	Sippican (United States)	RS-SDC	Carbon hygristor	0	0	1
VIZ	Sippican (United States)	Mark-II, Sippican II, VIZ-AIR, VIZ, VIZ-B, VIZ-B2, VIZ-II	Carbon hygristor	77	9.07	13
MEISEI	MEISEI (Japan)	MEIR91, RS016	Capacitive polymer	20	2.36	2
MRZ/Mars	AVK (Russian Federation)	MRZ, Mars	Goldbeater's skin	123	14.49	15
J/YANG	J/YANG (South Korea)	J/YANG	Carbon hygristor	3	0.35	1
IM-MK3	Indian Meteorological Service	IM-MK3	Carbon hygristor	35	4.12	3
Shang	Shanghai Radio (China)	Shang/E, Shang/M	Goldbeater's skin	90	10.60	7
MSS	Space Data Corporation (United States)	Meteorological Sounding System (MSS)	Carbon hygristor	4	0.47	1
ML-SRS	Meteolabor (Switzerland)	ML-SRS	Carbon hygristor, Snow White	1	0.12	0
Graw	Dr. Graw (Germany)	DFM90, DFM97	Capacitive	8	0.94	1
Modem	Modem (France)	GL98(capacity), M2K2	Capacitive	24	2.83	2
Total				849	100	169

TABLE 2. Matched stations where the dates of radiosonde type changes determined by the WMO reports are modified according to the time series of PW differences and other sources of radiosonde metadata.

GPS station	IGRA station No.	IGRA station name	Country for IGRA station	New type	Date (WMO reports)	Date (time series and others)	Old type
SASS	10184	Greifswald	Germany	VRS92-AGP	01 Feb 2006	01 Jun 2005	VRS80
LINZ	11010	Linz/Hoersching	Austria	VRS90L	01 Feb 2006	25 Sep 2005	VRS80
ISTA	17062	Istanbul/Goztepe	Turkey	VRS92G	01 Feb 2006	01 Jan 2005	VRS80
NKLG	64500	Libreville/Leonmba	Gabon	VRS80G	10 Jan 2002	11 Apr 2001	Mark-II
STJO	71801	St. Johns	Canada	VIZ B	Unknown	Dec 1992	
STJO	71801	St. Johns	Canada	VRS80	20 Apr 1998	01 Aug 1999*	VIZ B
AOML	72202	Miami	United States	VIZ-B2	Unknown	01 Jun 1997**	
AOML	72202	Miami	United States	RS80–57H	30 Nov 1996	01 Jun 1998**	VIZ-B2
RCM6	72202	Miami	United States	VIZ B	Unknown	07 Feb 1997**	
RCM6	72202	Miami	United States	VIZ-B2	Unknown	01 Jun 1997**	
RCM6	72202	Miami	United States	RS80–57H	30 Nov 1996	01 Jun 1998**	VIZ-B2
BRAZ	83378	Brasilia Aeroporto	Brazil	VRS92G	01 Feb 2006	27 Sep 2005	VRS80G
THTI	91938	Papeete/Tahiti	French Polynesia	VRS90G	10 Jan 2002	01 Apr 2001	VRS80G

* A combination of time series and the IGRA station history file.
** The change dates obtained from the NWS.

it would not introduce systematic errors for the large number of samples used here (Fig. 2).

For any comparison, the data quality of either dataset can contribute to the differences. Considerable effort has been made to improve the quality of both the radiosonde and GPS data. Durre et al. (2006) has described in detail the quality-control procedures applied to the IGRA dataset. In addition, we also put some criteria on radiosonde temperature and humidity profiles presented in section 2b to minimize the contribution from radiosonde missing data and the top of the profiles. Readers should be aware of the fact that the quality control of IGRA does not include bias adjustments of any kind, including known errors in temperature and humidity measurements. A series of quality checks have been applied to the GPS-derived PW and other parameters required for derivation of PW to lessen the error in the GPS PW. For individual matched stations, we also check the GPS log files on the IGS Web site (http://igscb.jpl.nasa.gov/) for any changes in ZTD that could lead to changes in PW. The artificial ZTD changes could result from occasional changes made by individual analysis centers (ACs) in their GPS data handling (e.g., different elevation cutoff angles, revised antenna phase maps) and their ZTD estimation algorithms (e.g., new mapping functions, different constraint schemes on the analysis parameters). Such changes are reduced by combining the ZTD solutions from seven ACs.

Errors in radiosonde and GPS data can also result in PW differences between them. Wang et al. (2007) did a thorough error analysis of the GPS PW dataset and found no systematic error and the random error of less than 3 mm. The possible systematic errors in the GPS PW data are associated with elevation cutoff angles and mapping functions used for deriving ZTD. The higher elevation angle can introduce a dry bias to the derived PW. Emardson et al. (1998) show that lowering the elevation angle from 15° to 10° can increase the GPS PW by 0–2 mm. Tregoning et al. (1998) found that the bias for the elevation angle from 10°–20° is less than 1.2 mm. Note that the 15° cutoff elevation angle was used by four ACs, and 7°, 10°, and 20° angles were used by the other three ACs (Gendt 1998). The ZTD solution we used is a combined solution of the ZTD values from all available ACs. Five out of all seven ACs use the mapping function from Niell (1996), which is not very accurate in the Southern Hemisphere and does not include mapping function variations on time scales less than one year. Tregoning et al. (1998) show that the Neil mapping function causes a dry bias of less than 1 mm in the PW estimates. In summary, the bias in the GPS PW data due to the elevation angles and the mapping functions is less than 3 mm and varies from one site to another depending on how many AC solutions are available and which ones are used for the final combined ZTD.

Although matched radiosonde and GPS stations are within 50 km horizontally, 100 m vertically, and 1 h temporally, there might still be discrepancies as a result of station separations because of the large variability of humidity both spatially and temporally. The difference from different measurement times between the radiosonde and GPS could well be random and could be cancelled out for a large number of samples. The impact of the elevation differences between radiosonde and GPS stations is negligible because no significant correlations are found between PW and elevation dif-

TABLE 3. Matched stations where at least one radiosonde type change has occurred. Radiosonde types and the time periods they were used are also given.

GPS	IGRA	IGRA station name	Country (IGRA)	Type 1	Type 2	Type 3
NYA1	01004	NY-Alesund II	Svalbard	RS80A 13 Apr 1998~30 Oct 2004	RS90 30 Oct 2004~30 Apr 2006	
NYAL	01004	NY-Alesund II	Svalbard	RS80A 01 Feb 1997~30 Oct 2004	RS90 30 Oct 2004~30 Apr 2006	
STAS	01415	Stavanger/Sola	Norway	RS80A 26 Jan 2003~01 Feb 2006	RS92 01 Feb 2006~30 Apr 2006	
VIS0	02591	Visby Aerologiska	Sweden	RS80A 24 Sep 2002~01 Feb 2006	RS92 01 Feb 2006~30 Apr 2006	
NEWL	03808	Camborne	United Kingdom	RS80H 27 Jun 2004~01 Feb 2006	RS92 01 Feb 2006~30 Apr 2006	
HERT	03882	Herstmonceux	United Kingdom	RS80H 08 Jun 2003~01 Feb 2006	RS92 01 Feb 2006~30 Apr 2006	
REYK	04018	Keflavik	Iceland	RS80A 01 Feb 1997~01 Feb 2006	RS92 01 Feb 2006~30 Apr 2006	
REYZ	04018	Keflavik	Iceland	RS80A 17 Aug 2003~01 Feb 2006	RS92 01 Feb 2006~30 Apr 2006	
KOSG	06260	De Bilt	Netherlands	RS80A 01 Feb 1997~10 Jan 2002	RS90 10 Jan 2002~02 Apr 2006	
VILL	08221	Madrid	Spain	RS80A 01 Feb 1997~01 Feb 2006	RS92 01 Feb 2006~30 Apr 2006	
CEUT	08495	North Front	Gibraltar	RS80H 22 Sep 2002~01 Feb 2006	RS92 01 Feb 2006~30 Apr 2006	
SASS	10184	Greifswald	Germany	RS80H 07 Sep 2003~01 Jun 2005	RS92 01 Jun 2005~30 Apr 2006	
GANP	11952	Poprad/Ganovce	Slovakia	RS90 19 Oct 2003~01 Feb 2006	RS92 01 Feb 2006~30 Apr 2006	
BOGI	12374	Legionowo	Poland	RS90 22 Sep 2002~01 Feb 2006	RS92 01 Feb 2006~30 Apr 2006	
BOGO	12374	Legionowo	Poland	RS80A 24 Jun 1999~10 Jan 2002	RS90 10 Jan 2002~01 Feb 2006	RS92 01 Feb 2006~30 Apr 2006
JOZ2	12374	Legionowo	Poland	RS90 17 Jul 2003~01 Feb 2006	RS92 01 Feb 2006~30 Apr 2006	
JOZE	12374	Legionowo	Poland	RS80A 24 Jun 1999~10 Jan 2002	RS90 10 Oct 2002~01 Feb 2006	RS92 01 Feb 2006~30 Apr 2006
WROC	12425	Wroclaw	Poland	RS90 22 Sep 2002~01 Feb 2006	RS92 01 Feb 2006/30 Apr 2006	
BUTE	12843	Budapest/Lorinc	Hungary	RS90 31 Oct 2004~01 Feb 2006	RS80A 01 Feb 2006~30 Apr 2006	
BUCU	15420	Bucaresti/Bancasa	Puerto Rico	RS80A 13 Apr 2000~10 Jan 2002	RS90 10 Oct 2002~30 Apr 2006	
ISTA	17062	Istanbul/Goztepe	Turkey	RS80A 07 Apr 2000~01 Jan 2005	RS92 01 Jan 2005~28 Apr 2006	
STJO	71801	St. Johns	Canada	VIZ 01 Feb 1997~01 Aug 1999	RS80A 01 Aug 1999~30 Apr 2006	
AOML	72202	Miami	United States	VIZ 22 Feb 1998~01 Jun 1998	RS80H 01 Jun 1998~04 Apr 2004	
RCM6	72202	Miami	United States	VIZ 07 Feb 1997~01 Jun 1998	RS80H 01 Jun 1998~23 Sep 1998	
USN3	72403	Sterling	United States	RS80H 28 Jul 2004~01 Aug 2005	VIZ 01 Aug 2005~30 Apr 2006	
USNO	72403	Sterling	United States	RS80H 11 Jun 1997~01 Aug 2005	VIZ 01 Aug 2005~29 Apr 2006	
BRAZ	83378	Brasilia Aeroporto	Brazil	RS80A 02 Feb 1997~27 Sep 2005	RS92 27 Sep 2005~09 Mar 2006	
CAS1	89611	Casey	Antarctica	RS80A 01 Feb 1997~01 Feb 2006	RS92 01 Feb 2006~30 Apr 2006	
NOUM	91592	Noumea	New Caledonia	RS80A 22 Feb 1998~10 Jan 2002	RS90 10 Jan 2002~01 Feb 2006	Modem 01 Feb 2006~30 Apr 2006
THTI	91938	Papeete/Tahiti	French Polynesia	RS80A 17 Jun 1998~01 Apr 2001	RS90 01 Apr 2001~01 Feb 2006	Modem 01 Feb 2006~30 Apr 2006
AUCK	93112	Whenuapai	New Zealand	RS80A 06 Feb 1998~01 Feb 2006	RS92 01 Feb 2006~30 Apr 2006	
DARW	94120	Darwin	Australia	RS80A 01 Jun 1999~01 Jan 2006	RS92 01 Jan 2006~30 Apr 2006	
COCO	96996	Cocos Island	Cocos Island	RS80A 01 Feb 1997~23 Nov 2005	RS92 23 Nov 2005~29 Apr 2006	

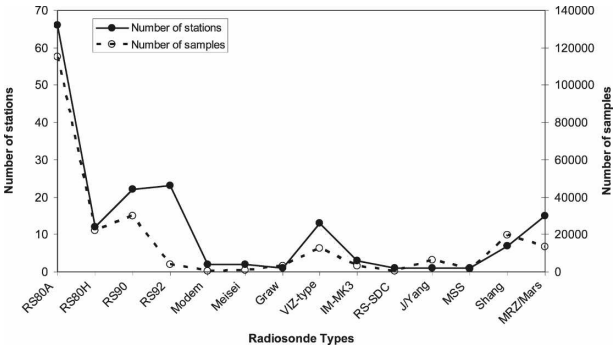

FIG. 2. Total number of stations (solid line) and samples (data points, dashed line) for each of 14 radiosonde types in the matched dataset.

ferences. The horizontal separation could introduce systematic differences in PW if GPS and radiosonde stations have very different humidity structures in spite of the small distance between the two stations. Wang et al. (2006) show one example in La Jolla, California, where the radiosonde and GPS stations are only 8 km apart but the local unique feature of a strong near-surface inversion at the radiosonde station is most likely absent at the GPS station and thus leads to a large discrepancy in PW. Gutman et al. (2004) also gave an example of a PW comparison between a radiosonde and two nearby GPS sites near Sterling, Virginia, and found that good agreement is achieved for the GPS station located downwind of the radiosonde site. To limit this kind of problem, we used Google Earth to check accurate locations for matched stations and their associated terrain for any possible effects of the horizontal separation. We found that at seven stations situated in the coastal regions, mean PW differences are two or more times their standard deviations (representing random errors), which can be qualitatively explained by their location dissimilarities. In those regions, sharp gradients exist in the meteorological parameters including PW. The location separation is considered in the following discussions of comparison results.

3. Comparison results

This section presents comparison results from matched radiosonde and GPS PW data at 169 stations from February 1997 to April 2006 for 14 radiosonde types (Figs. 1 and 2). Note that PW difference and PW bias hereafter in the text and the figures are all defined as radiosonde PW minus GPS PW. Based on the discussions in section 2c, the GPS PW can be used as a reference for the following discussions. However, any GPS-related factor that could be attributed to the PW differences is also considered. The comparison results are organized to show systematic PW errors of the 14 radiosonde types along with their characteristics, examples of using the time series of PW differences to identify any changes (both hardware and software) affecting radiosonde humidity measurements, and finally diurnal sampling errors for once- and twice-daily radiosonde data.

a. Measurement biases and their characteristics

Mean PW differences (IGRA minus GPS) for all available data points are shown in Fig. 3. For the seven types of radiosondes using capacitive humidity sensors (RS80A, RS80H, RS90, RS92, Modem, Meisei, and Graw), 103 out of a total of 128 stations show that, on average, the radiosonde PW is smaller than the GPS PW. Previous studies have discovered the dry bias of the Vaisala Humicap and the Meisei capacitive humidity sensor (cf. Wang et al. 2002a; Nakamura et al. 2004). However, a majority of stations launching radiosondes with carbon hygristors and goldbeater's skins exhibit moist biases. The moist bias in the carbon hygristor measurements was identified in Wade and Schwartz (1993) and Ciesielski et al. (2003), and is predominantly at the low levels (below 750 hPa). The latter would result in a moist bias in PW. The moist bias in the goldbeater's skin sensor is most likely due to its slow response and the general decrease of specific humidity with height. The PW differences for the Indian radiosonde, IM-MK3, bear the largest standard deviation, while the Vaisala RS92 shows the smallest standard deviation. The standard deviation of the differences is a good representation of the radiosonde random error. Figure 3 also gives the mean and standard deviation values averaged for stations using three types of hygrometers. Averaged systematic and random errors for capacitive, carbon hygristor, and goldbeater's skin hygrometers are −1.19/1.01/0.76 and 1.74/3.63/2.08 mm, respectively. Although various factors discussed in section 2c can contribute to the PW differences, the dependence of PW differences on radiosonde type is indisputable. In addition, the biases shown in Fig. 3 for three types of radiosonde hygrometers are consistent with previous findings. We have also tested whether mean differences shown in Fig. 3 are significantly dissimilar from 0 mm using the Student's t test. The stations with statistically significant biases are labeled with small red dots in Fig. 3; 106 stations show significant bias.

Variations of absolute and relative PW differences with the GPS PW are shown in Figs. 4 and 5 for eight radiosonde types that are used in more than three sta-

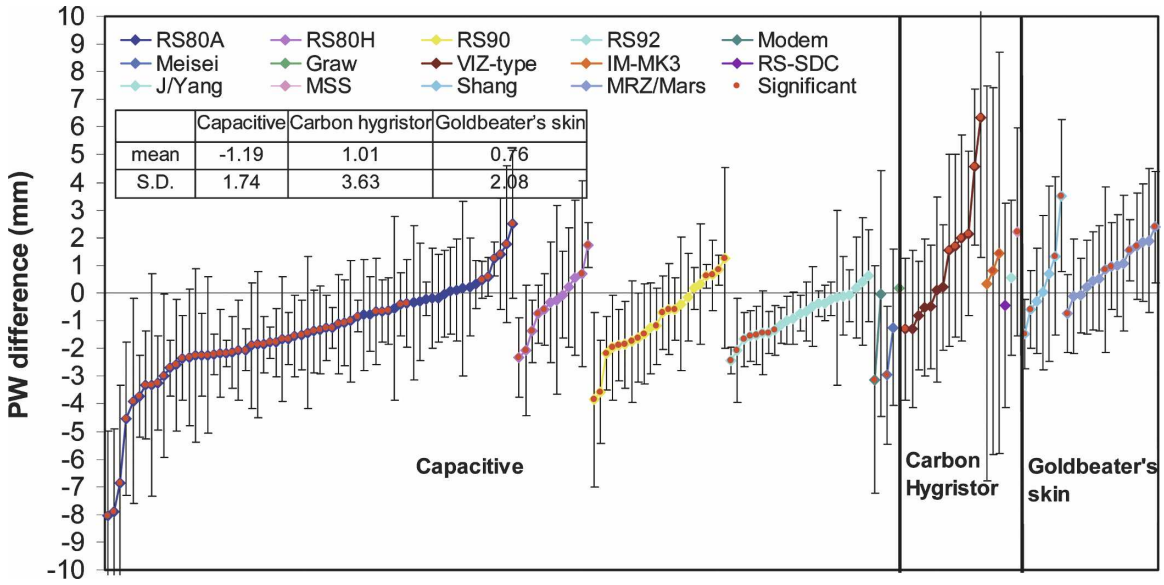

FIG. 3. Mean values (mm) and standard deviations (mm) of PW differences (IGRA minus GPS) at 169 stations for 14 radiosonde types. The stations are grouped into three based on their humidity sensor type. For each radiosonde type, the stations are sorted from the minimum to maximum mean values. The small red dots mark mean values significantly different from zero (i.e., the bias is statistically significant). Averaged mean and standard deviation values are given for three types of humidity sensors in the table.

tions in our data sample (see Table 2). The relative difference is defined as the PW difference (IGRA − GPS) divided by the GPS PW and is expressed as percentage in Figs. 4 and 5. The PW dry bias in the RS80A data is evident for the full range of PW values (0–70 mm) and increases linearly with PW, while the relative bias stays roughly constant and is less than 10% at PW $>$ 10 mm (Fig. 4). The large mean and standard deviation of relative differences for the first PW interval (0–2 mm) are sometimes misleading because of very small PW values and so are not plotted in Fig. 4. The RS80H, RS90, and RS92 exhibit similar characteristics, the pronounced dry bias for PW $<$ 40 mm and the general increase of relative biases for the PW of ~5–40 mm. This is not surprising because they all use the H-Humicap. The RS92 sensor seems to have the best performance with the smallest mean bias and standard deviation. The averaged moist bias of the VIZ-type radiosonde primarily occurs at PW between 15 and 60 mm and is less than 3 mm (~10%; Fig. 5). However, the IM-MK3, which also carries the carbon hygristor, displays very different variations: a much larger moist bias at PW $<$ 40 mm and the largest random errors (standard deviation; Fig. 5). The moist bias at PW $<$ 12 mm for the IM-MK3 is enormous (larger than 50%; Fig. 5). The poor performance of Indian radiosondes also appears in the temperature data and shows large random errors and large heterogeneities (e.g., Elms 2003; Kuo et al. 2005; Thorne et al. 2005). The WMO report (Elms 2003) found that the random errors of geopotential heights for the IM-MK3 were the largest for any major radiosonde type. It suggests that the performance of the IM-MK3 is very unstable. The Shang and MRZ/Mars radiosondes, both of which use goldbeater's skin, show small moist biases (<2 mm) and less consistent variations with PW (Fig. 5).

The dry bias in the Vaisala radiosonde humidity data has been well documented by previous studies (see the summary in Häberli 2006). A new protective shield over the humidity sensor boom was introduced to the Vaisala RS80 series and was expected to prevent the contamination dry bias (Wang et al. 2002a). Several preliminary studies have evaluated the impact of the new sensor boom cover (Wang 2002; Nakamura et al. 2004). Figure 6 presents the variations of the mean PW differences (IGRA minus GPS) with the GPS PW for the RS80A and RS80H radiosondes using data from 2000 and 2001. The new sensor boom cover clearly reduces the RS80A dry bias by ~2%; however, a dry bias of 4% in PW still remains in the RS80A data. This agrees with a few early studies (Fujiwara et al. 2003; Wang 2002; Nakamura et al. 2004). The impact of the sensor boom cover on the RS80H radiosonde changes the dry bias to a small moist bias at PW $>$ 20 mm (Fig. 6). Figure 6 also shows whether mean PW difference for each bin is statistically significantly different between 2000 and 2001 data. For RS80A, 26 out of total 32 bins have significant changes in PW difference from 2000 to

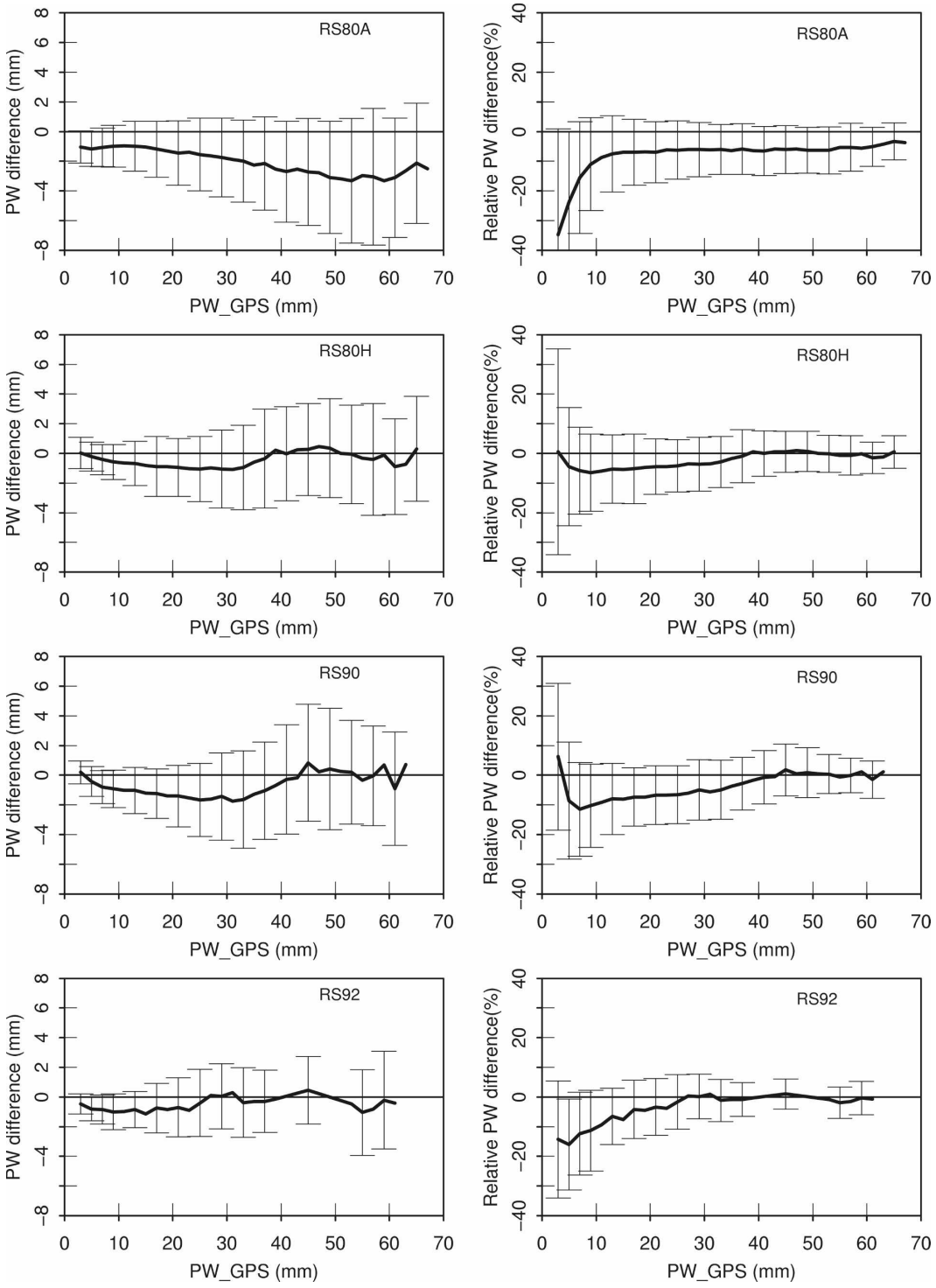

FIG. 4. Averaged (left) absolute (mm) and (right) relative PW differences as a function of GPS PW in each 2-mm PW bin for Vaisala RS80A, RS80H, RS90, and RS92. The standard deviation in each bin is also given in error bars.

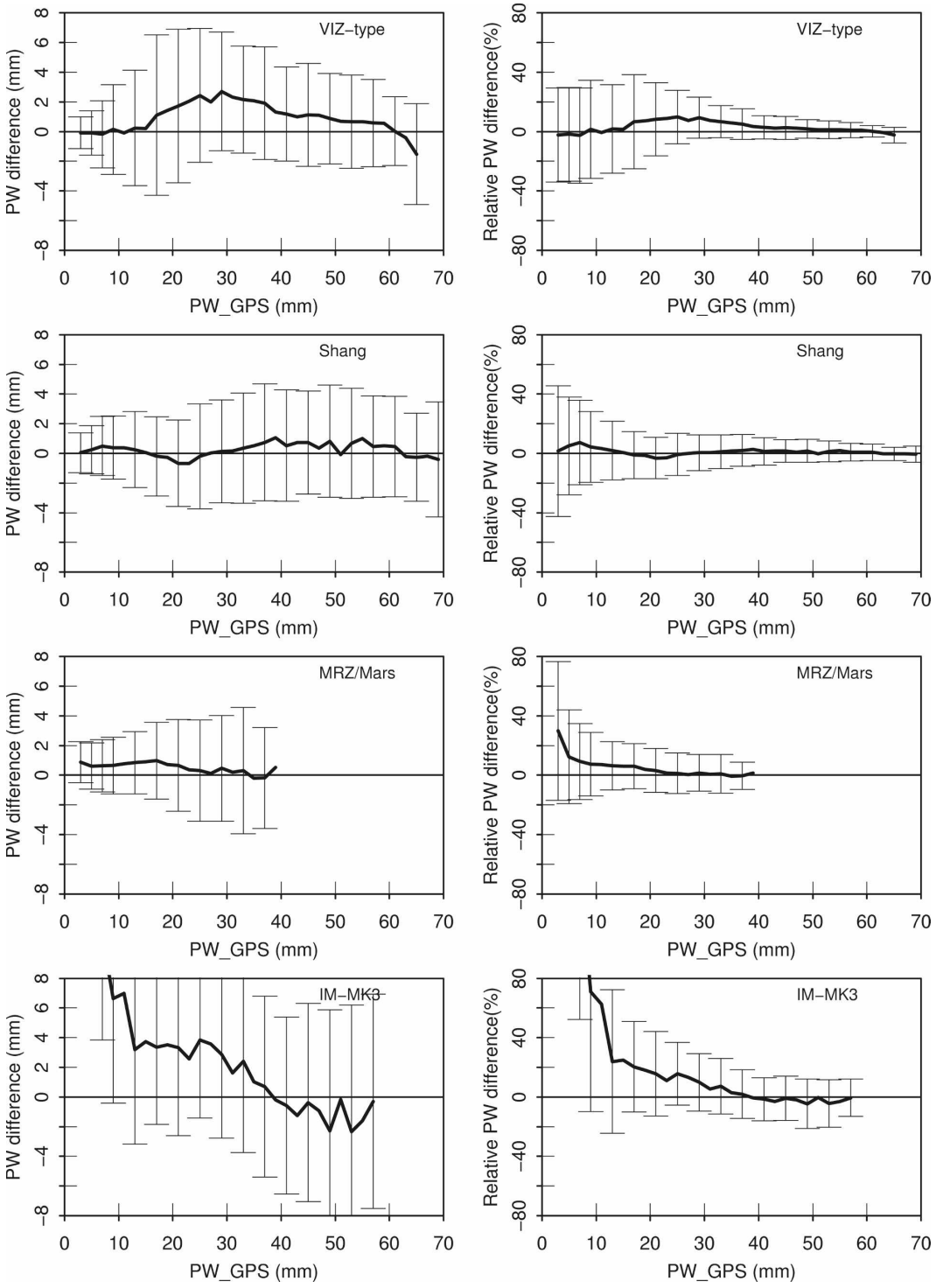

FIG. 5. As in Fig. 4, but for VIZ-type, Shang, MRZ/Mars, and IM-MK3 radiosondes.

2001. For RS80H, the change for PW below 20 mm is generally not significant.

There have been a number of studies on the day–night differences of the radiosonde humidity bias, especially for the Vaisala Humicaps (e.g., Wang et al. 2002a; Van Baelen et al. 2005). The larger dry bias during daytime is primarily a result of solar radiation heating of the humidity sensor arm both prior to launch

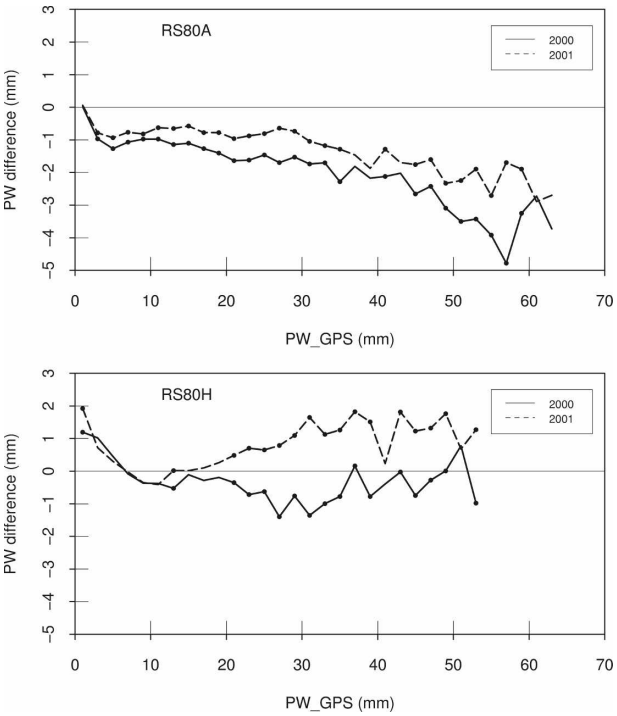

FIG. 6. Mean PW differences (mm) as a function of GPS PW for (top) RS80A and (bottom) RS80H using data in 2000 (without the sensor boom cover; solid line) and 2001 (with the sensor boom cover; dashed line). Note that only the data at stations that have both 2000 and 2001 data available are included in this analysis. The significant points are marked with dots.

and during flight (Wang et al. 2002a; Vömel et al. 2007). Figure 7 shows comparisons for the frequency distributions of PW differences between daytime and nighttime for eight radiosonde types. The larger dry bias of the Vaisala radiosondes during daytime compared to nighttime is evident in Fig. 7 and is manifested by the shift of the center of the peak frequency without changes in the shape of the frequency distribution. Mean day–night differences are statistically significant for all eight types. The magnitude of the day–night difference is larger for the RS90 and RS92 than for the RS80A and RS80H. An aluminized plastic protective cap is installed over the RS80 humidity sensor to reduce the solar radiation heating of the Humicap and to prevent contamination by rain and ice. The RS90 and RS92 humidity sensors have two alternately heated H-Humicaps without the radiation/rain shielding cap, which makes them more susceptible to solar radiation. Vömel et al. (2007) found that the average solar radiation dry bias of the Vaisala RS92 humidity sensor is on the order of 9% at the surface for solar zenith angles between 10° and 30°. During the WMO radiosonde intercomparison project in Vacoas, Mauritius, in 2005, the day–night difference of 3%–7% in Vaisala relative humidity measurements was also found in radiosonde intercomparisons, and was confirmed by the comparison with the GPS PW data collected in the project (Nash et al. 2005). We found that the average relative PW dry bias for the RS92 is 10% and 5% during daytime and nighttime, respectively (not shown). Figure 7 also suggests that the moist bias during daytime is slightly greater than that during nighttime for the VIZ-type, Shang, MRZ/Mars, and IM-MK3 sensors. Approximately normal distributions of PW differences are shown for all radiosonde types except the IM-MK3, which has a much wider distribution with more than 20% of the data points falling beyond −7.5–7.5 mm.

b. Long-term temporal inhomogeneity

The artificial temporal inhomogeneity (i.e., discontinuity) of radiosonde data introduced by changes in radiosonde types and data collecting and processing procedures has been the most serious problems for climate studies. This section is devoted to understanding temporal changes of PW differences between radiosonde and GPS at each station and to finding out whether they can be used to detect the artificial changes in radiosonde PW. Problems in the GPS data might still exist in spite of the efforts described in section 2c to identify and minimize the temporal inhomogeneity in the GPS PW data. Therefore, it is necessary to be very careful not to simply interpret the changes in time series of PW differences presented below as the temporal inhomogeneity in radiosonde data. For the time series at each station, we visually examine the time series of both PW from each dataset and their differences to discover which data contribute to the discontinuity in the PW difference. Monthly mean PW differences from February 1997 to April 2006 are calculated using all matched data points, with a requirement of at least 20 samples each month, and are presented for five stations in Fig. 8.

1) At Churchill, Manitoba, Canada, the Vaisala RS80A radiosonde has been launched from 1997 to the present. The comparison shows the consistent dry bias of less than 2 mm throughout the period, and suggests a slightly smaller dry bias starting in 2001, especially in the summer (Fig. 8). The latter feature might be due to the effect of the contamination protective shield over the humidity sensor that was introduced for the Vaisala RS80 radiosonde in late 2000, which is consistent with the data shown in Fig. 6.
2) Several striking features are displayed at Miami, Florida, where the VIZ-B2 and RS80H were used before and after 1 June 1998, respectively (Elliott et

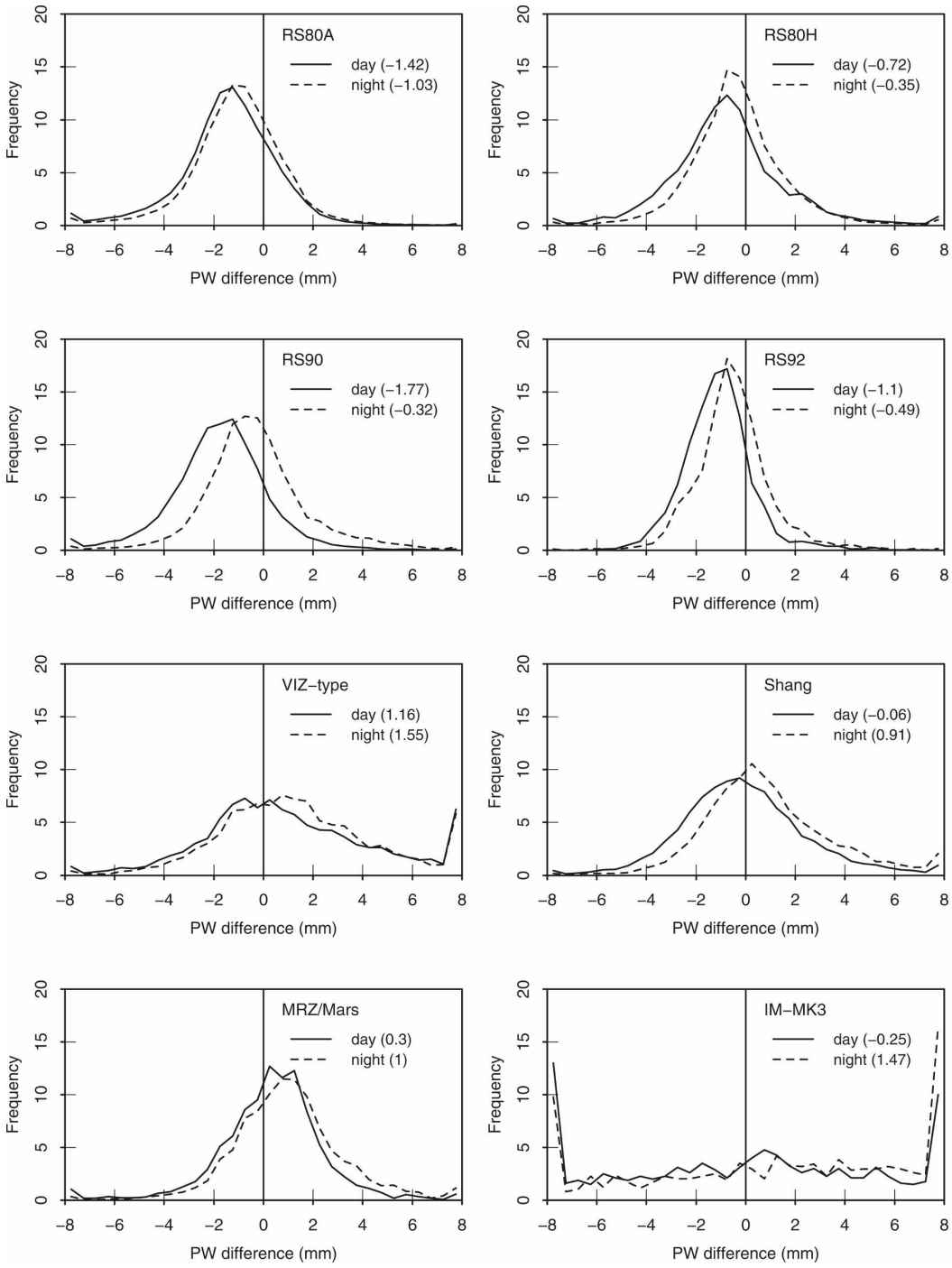

FIG. 7. Comparisons of the frequency (%) distributions of PW differences (mm) between daytime and nighttime for eight radiosonde types. The mean value (mm) for each case is given in the legend.

al. 2002). The VIZ-B2 shows a large and coherent moist bias (>3 mm) and is likely due to the moist bias of the carbon hygristor. A dry bias is present after the transition to the RS80H until 2001 and is most pronounced in 1999, which can be explained by the RS80H's dry bias. The systematic moist bias starting in 2001 for RS80H in Fig. 8 might be due to the introduction of the protective shield over the humidity sensor as shown in Fig. 6 and discussed in section 3a.

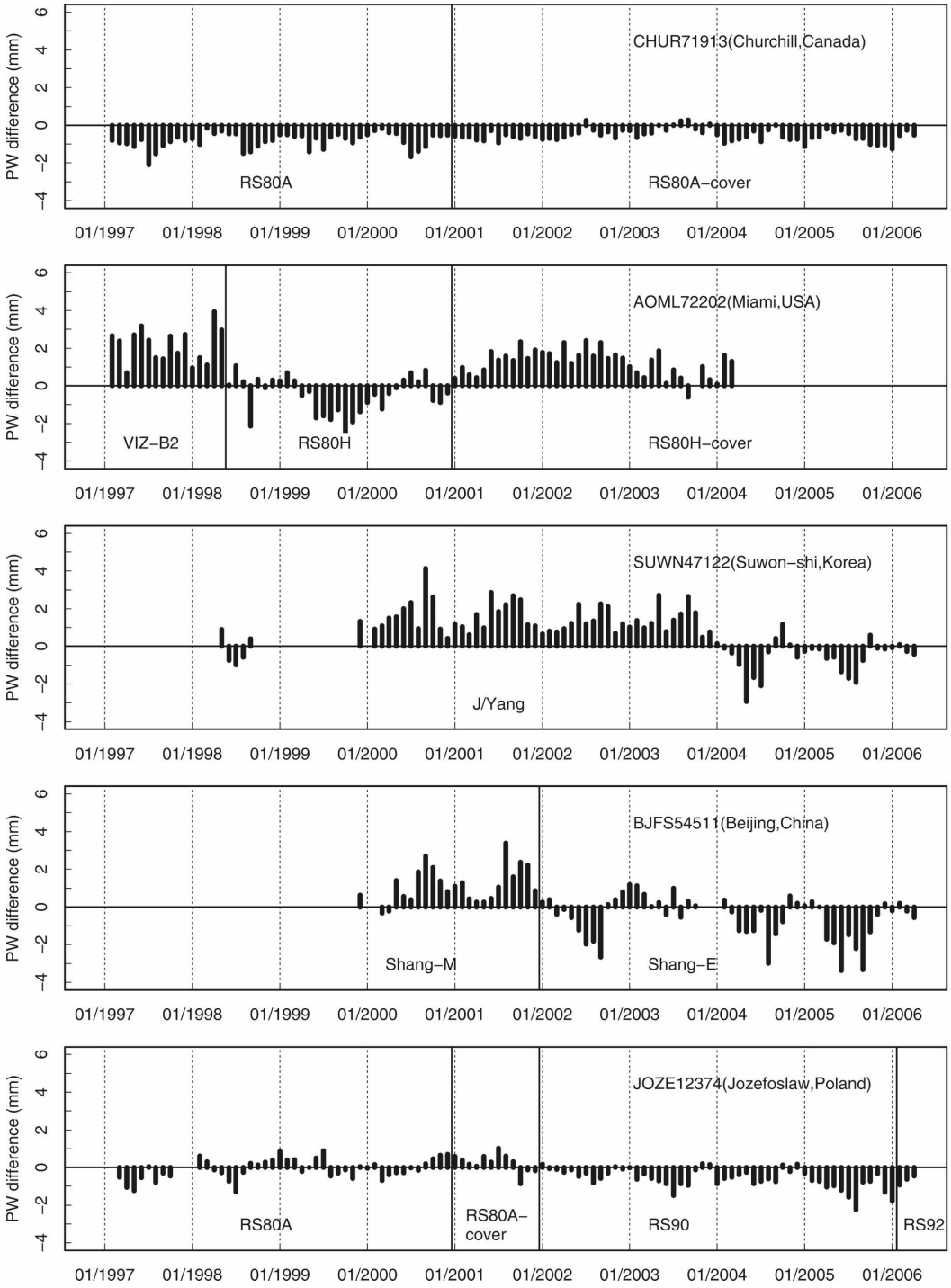

FIG. 8. Monthly mean PW differences (mm) from 1997 to 2006 at five matched stations. The station identifications and names are shown in the upper-right legend. The radiosonde types are separated by vertical solid lines and given in the lower part. The RS80-cover means the RS80 radiosondes with the new sensor boom cover introduced in 2001.

3) At Suwon-shi, South Korea, the WMO reports from 1996 to 2006 have not stated any radiosonde type change. However, the comparison shows a clear transition from the moist bias before January 2004 to the dry bias afterward. It remains unclear why such a transition occurred.
4) At Beijing, China, the old mechanical Shang radiosonde (referred as Shang-M) was launched before

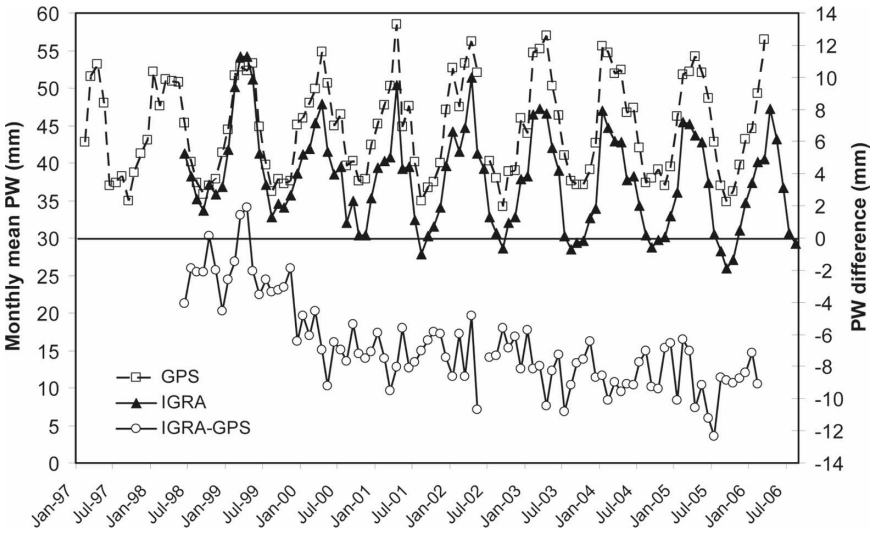

FIG. 9. Monthly mean PW from the IGRA (solid line with diamond) and GPS (dashed line with square) data at Fortaleza, Brazil. Monthly mean PW difference (IGRA minus GPS) is in solid line with circle and uses the *y* axis on the right.

2002. The new digital Shang radiosonde (referred as Shang-E) started to fly operationally in Beijing in January 2002 and uses a rod thermistor, a carbon hygristor, and a silicon pressure sensor in contrast to the bimetallic strip, goldbeater's skin, and aneroid capsule for the Shang-M. Figure 8 shows the change from the positive bias in the Shang-M data to the general negative bias in the Shang-E data.

5) At Jozefoslaw, Poland, the Vaisala RS80A was used from 1997 to 2001, the RS90 during 2001–05, and the RS92 starting in February 2006. The RS80A did not show a consistent bias during the 5-yr period, whereas the RS90 shows the systematic dry bias with a maximum in summer.

Any artificial inhomogeneity in the data can lead to inaccurate trend estimates. Figure 9 shows monthly-mean PW values from the IGRA and GPS PW data at Fortaleza, Brazil. The radiosonde (WMO 82397) and GPS (FORT) stations are 22 km apart. During the 10-yr period, the Vaisala RS80A was launched at the radiosonde site, although it should be noted that the new sensor boom cover was introduced to RS80A in 2001 (see discussions in section 3a). Two datasets show very good agreement on the regular seasonal cycle of ~15–20 mm amplitude and the year-to-year variations. Nevertheless, monthly mean radiosonde PW values are smaller than that from the GPS PW dataset, which is consistent with the well-known dry bias for the Vaisala RS80. More importantly, the magnitude of the dry bias increases with time from less than 5 mm before 2000 to larger than 6 mm in 2005 (Fig. 9). A conical radome was used from 1997 to 27 February 2006 at the FORT IGS station (Ray et al. 2006). The addition of a radome produces an error in the station height, which in turn causes an error in zenith wet delay (ZWD; −0.4 times the height error) and in PW (~0.15 of the ZWD error; Niell et al. 2001). The height error of the radome at FORT is estimated to be a downward bias of ~16 mm (Ray et al. 2006), which corresponds to a positive bias of about 0.96 mm in PW. Before the FORT site decommission on 8 April 2006, the radome was removed starting on 27 February 2006 in order to study the effect of the radome by comparing the data without the radome with the data from the new replacement site BRFT. Our PW comparison at FORT and BRFT from 27 February to 8 April 2006 concludes that the radome introduces a mean wet bias of 0.92 mm, which is comparable to the 0.96 mm bias estimated above from the height bias. The ~1-mm wet bias of the GPS PW is not enough to explain the difference between the radiosonde and GPS and its variation with time shown in Fig. 9. Therefore, it is not clear what causes the increase of the dry bias in the radiosonde data in 2000 shown in Fig. 9. Monthly mean PW anomalies (with a five-point running mean) from the IGRA data indicate a strong negative PW trend during this period, while the GPS PW data show a small positive trend (Fig. 10). Although the calculated linear trend bears uncertainties because of the short data record, the discrepancy in the sign of the trend between the radiosonde and GPS data is unquestionable. This example clearly demonstrates the significant impact of artificial inhomogeneity in the climate

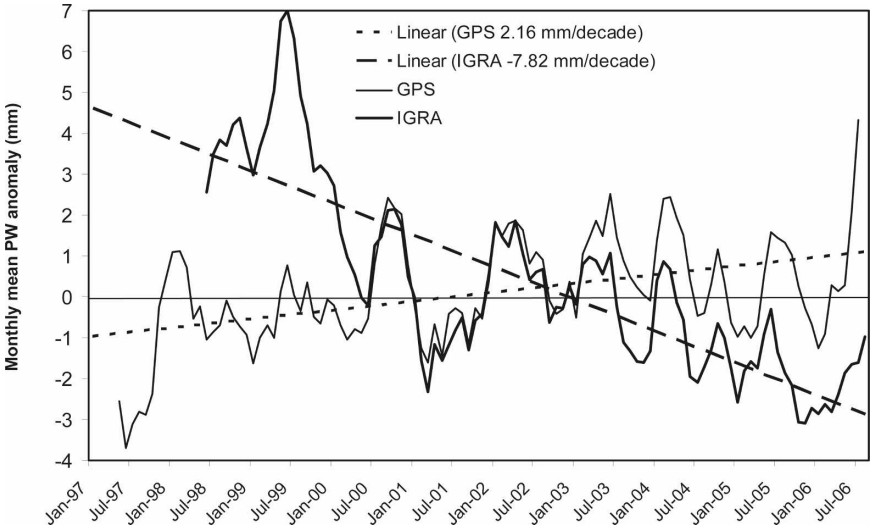

FIG. 10. Monthly mean PW anomaly from the IGRA (thick line) and GPS (thin line) data at Fortaleza, Brazil. The linear trend lines are given in dashed lines. A five-point running mean has been applied to monthly mean anomaly. The linear trend in mm decade^{-1} is shown in the legend.

data on the trend analysis. What matters most for the climate trend analysis are changes in the systematic errors of the radiosonde data.

c. *Diurnal sampling errors*

Based on WMO (2006), 501 of the global 788 radiosonde stations launch sondes at 0000 and 1200 UTC, 137 only at 0000 UTC, 128 at 1200 UTC, and 22 more than twice daily (Fig. 11). The stations only collecting wind data are excluded in Fig. 11. It should be noted that the accuracy of the information presented in Fig. 11 is open to question (T. Oakley 2007, personal communication). The majority of stations routinely launching sondes at 0000 UTC are in the Western Hemisphere, while most of the stations in South and Central America only launch sondes at 1200 UTC (Fig. 11). The once- or twice-daily sampling is not high enough to capture the whole diurnal cycle. The impact of diurnally undersampling the atmosphere on the monthly-mean climatology depends on the diurnal amplitude and phase of the studied parameter. In this section, we estimated the diurnal sampling errors of once- and twice-daily radiosonde PW data by comparing the PW seasonal means calculated from the 2-yr (2003–04) twice-daily (0100 and 1300 UTC) and once-daily (0100 or 1300 UTC) GPS PW data with those from the original 2-hourly PW data. Note that the GPS PW data are available at odd hours (0100, 0300, . . . , 2300 UTC). The 0100 and 1300 UTC GPS data are used to represent the 0000 and 1200 UTC radiosonde launch times. The diurnal sampling error in percentage is expressed as the difference in PW divided by the seasonal mean computed from the 2-hourly data.

Figure 12 shows the annual mean sampling errors at 220 stations for twice- and once-daily radiosonde data. The annual mean sampling errors are generally small (within $\pm 2\%$) for the twice-daily data, but can be as high as 10%–15% and have magnitudes larger than 2% at 33% of the stations for the once-daily data (Fig. 12). The sampling errors for only the 0100 UTC data are negative at most of the global stations (75% of the stations) except in South America where the large positive biases are shown (Fig. 12). The errors of only the 1300 UTC data are generally the opposite of those for only the 0100 UTC data, with positive biases at 69% of the stations. The general pattern for the signs of the sampling errors for the once-daily radiosonde data varies insignificantly with seasons (not shown). As shown in Fig. 12 of Wang et al. (2007), the Darwin region has a very large PW diurnal cycle with the peak-to-peak amplitude larger than 2 mm and the minimum and maximum values at ~0900 and ~2100 LST (0100 and 1300 UTC), respectively. As a result of such a PW diurnal cycle, the soundings at 0000 and 1200 UTC would produce the negative and positive biases to the PW, respectively (Figs. 12b,c). However, the twice-daily sounding at 0000 and 1200 UTC would capture the peak and dip in the PW, simulate the diurnal cycle well, and cause a negligible diurnal sampling error (Fig. 12a). Because of the spatial variations of radiosonde launching times (Fig. 11) and diurnal sampling errors (Fig. 12),

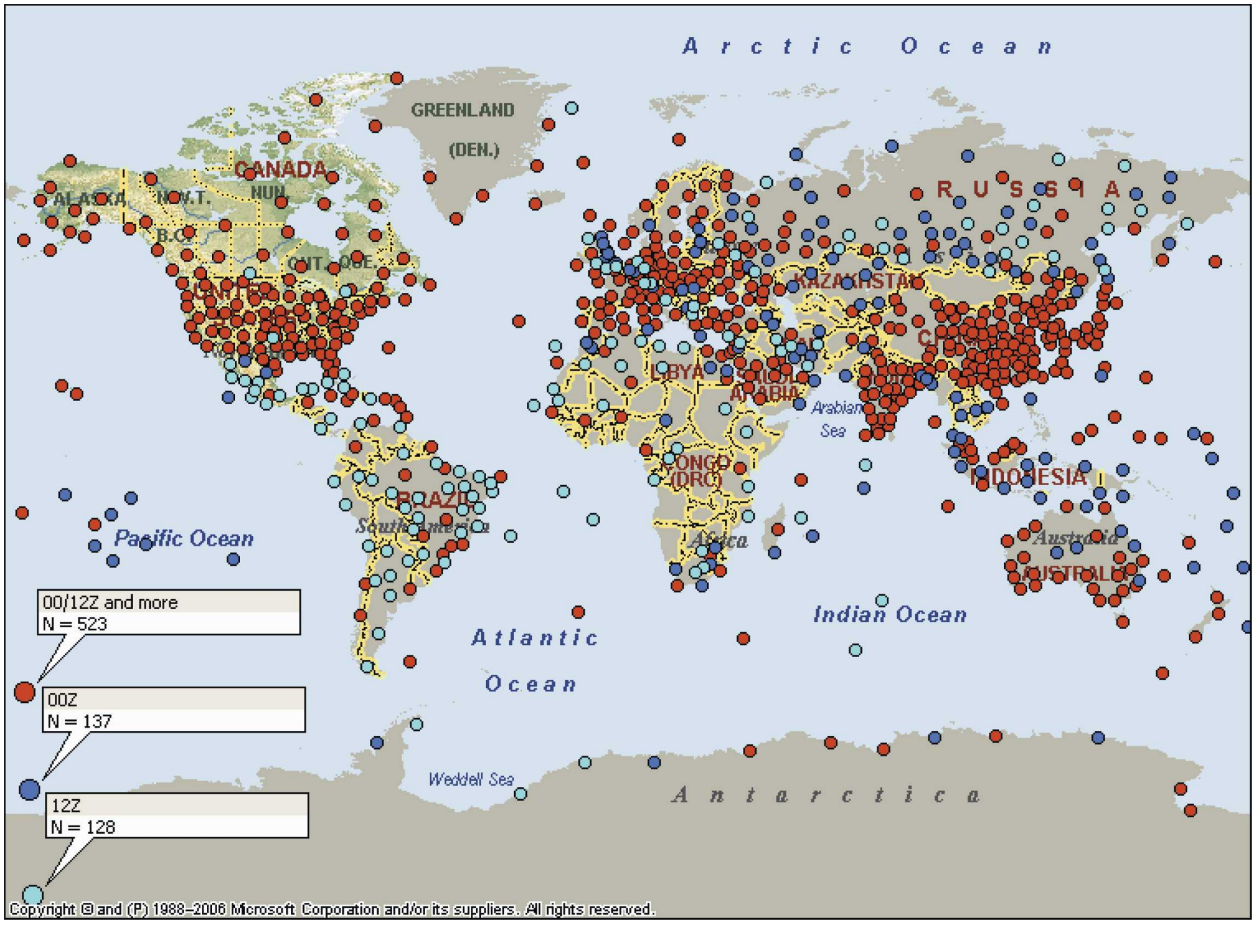

FIG. 11. Radiosonde launch times at 788 stations. Stations launching sondes at 0000, 1200, and more UTC are in red. Dark and light blues show stations launching sondes at 0000 and 1200 UTC, respectively.

global radiosonde PW data would have very small diurnal sampling errors in some parts of the world and systematic errors in other parts, such as the negative bias in South America where only one sounding per day at 1200 UTC is launched.

4. Summary and discussion

A global radiosonde PW dataset (IGRA) has been compared with a global GPS PW dataset from 1997 to 2006 by matching the data in space and time. A total 130 pairs of radiosonde and GPS stations have been found within 50 km in horizontal distance and 100 m in elevation and include 14 types of radiosondes. The GPS-derived PW is considered as a reference because of its high accuracy and long-term stability. The radiosonde/GPS PW comparisons show systematic PW errors for 14 radiosonde types, their characteristics, the temporal inhomogeneity as a result of radiosonde type and other alterations, the impact on climate trend detection, and the diurnal sampling errors. The findings are summarized below.

- Measurement biases and their characteristics.
  The 14 types of radiosondes studied here employ three different types of humidity sensors: capacitive polymer, carbon hygristor, and goldbeater's skin. The stations using sondes with a capacitive sensor have a mean dry bias of 1.19 mm with a standard deviation of 1.74 mm, while those using a carbon hygristor and goldbeater's skin have a mean moist bias of less than 1 mm with a standard deviation of 2–3.7 mm. The Vaisala RS80A's PW dry bias roughly increases linearly with PW in absolute value and ~8% in relative value for PW > 10 mm. The dry bias for the Vaisala RS80H, RS90, and RS92 data is smaller than that for the RS80A data and primarily occurs over the PW range of ~5–40 mm. For the four kinds of Vaisala radiosondes, the newest version, the RS92, has the best performance. The bias variations in the VIZ-

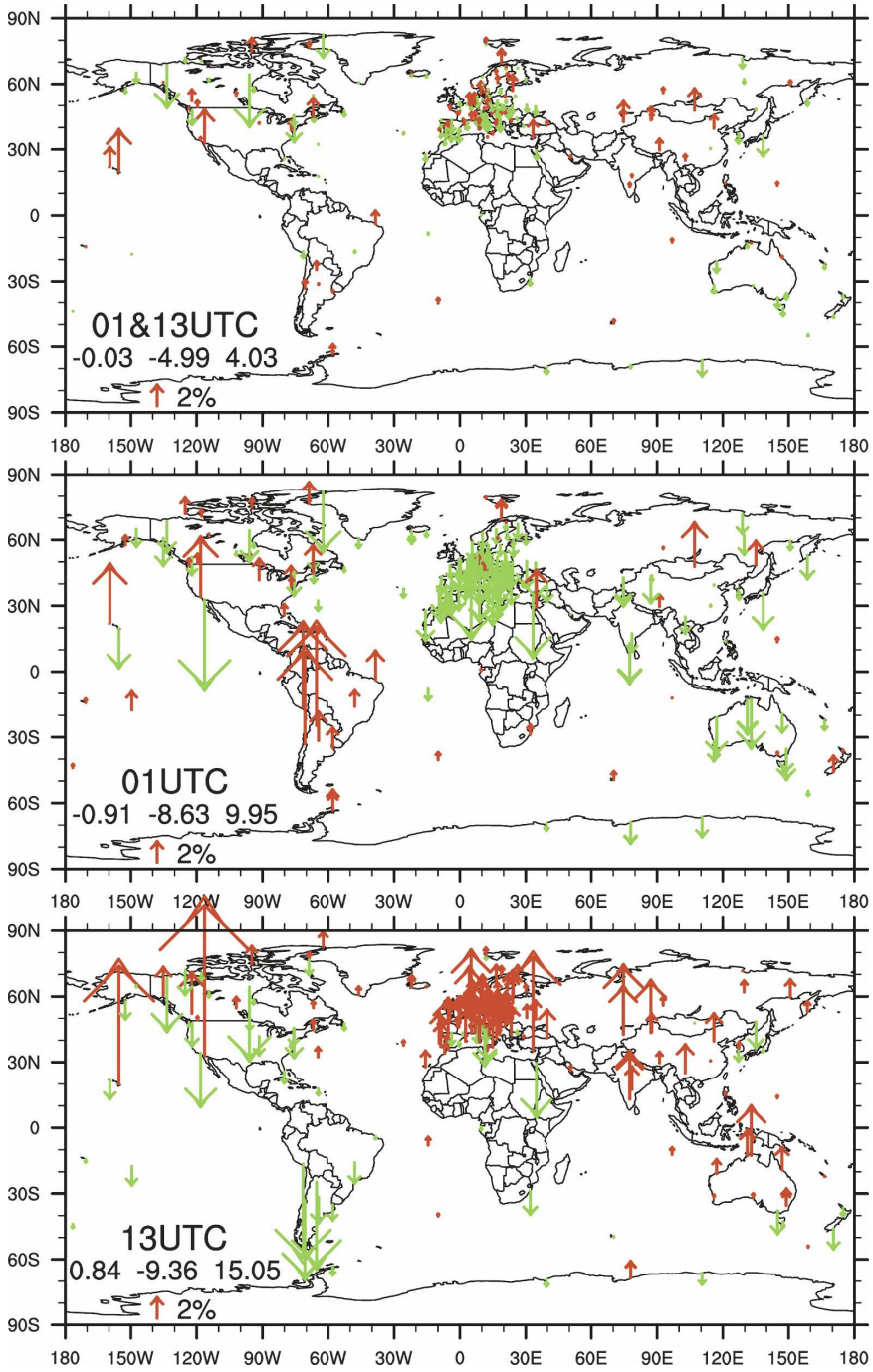

FIG. 12. Annual mean diurnal sampling errors (%) for twice-daily (0001 and 1300 UTC) and once-daily (0001 or 1300 UTC) soundings. The red upward arrows symbolize positive errors, and the green downward arrows represent negative errors. The length of the arrow represents the magnitude of the errors. Mean, minimum, and maximum values are provided in the legend.

type, Shang, and MRZ/Mars with PW are small. The IM-MK3 has a moist bias at PW values below 40 mm, and it also has the largest random error. The new humidity sensor boom cover, introduced in late 2000, for the Vaisala RS80 radiosonde series reduces the RS80A's dry bias by ~2%, from 6.1% in 2000 to 3.9% in 2001, and also changes the RS80H's bias from −2.6% in 2000 to +1.1%. The dry bias for the

Vaisala radiosondes is larger during daytime than nighttime, and the day–night difference is more profound for the RS90 and RS92 than for the RS80A and RS80H.

- Long-term temporal inhomogeneity.
  Monthly mean PW differences between the radiosonde and GPS from February 1997 to April 2006 are shown at five stations in Fig. 8. The discontinuities associated with transitions from one radiosonde type to another can be identified in the time series. However, some of the temporal variations of PW differences cannot be explained and need to be investigated more at a later time. One example is given to show that artificial temporal inhomogeneity in the climate data record can lead to an inaccurate climate trend estimate; sometimes it can even produce a wrong sign for the climate trend.
- Diurnal sampling errors.
  The diurnal sampling error for the twice- and once-daily radiosonde data is estimated by sampling the 2-hourly GPS PW data at radiosonde launch times. The sampling error for twice-daily soundings is generally small (±2%); however, it can be as much as 10%–15% for the once-daily data. The sampling error for the 0100 UTC data is negative at most of stations, and is generally opposite to that of the 1300 UTC data. As a result of spatial variations for the radiosonde launching times and diurnal sampling errors, the magnitude and sign of the diurnal sampling errors for the actual global radiosonde data will also vary in space.

Several types of systematic errors in the global radiosonde PW data have been revealed based on comparison with the independent GPS PW data. The findings clearly demonstrate the importance of independent, redundant, and collocated observations for a single meteorological parameter for identification, quantification, and possible correction of systematic errors in the data. During this study, we also found that the following factors complicate the explanation of the differences between two instruments, and we would like to make recommendations for future needs of radiosonde and GPS PW data.

- A small spatial separation for the radiosonde and GPS stations could bring about a significant PW difference, especially in the regions where strong PW gradients exist. In the future, it is very important to collocate GPS and radiosonde stations. Such a collocation is beneficial to both GPS data processing and radiosonde data quality control. Radiosonde data can be used to derive the mapping function for the GPS data processing; GPS data are very useful for monitoring the quality of the radiosonde humidity data both in real time and in postprocessing.
- Comprehensive metadata documentation for any changes in, for example, instrumentation and data processing, are lacking for both the radiosonde and GPS data. The metadata would be very helpful in explaining the significant variations in the time series of PW differences and would help in determining which data could contribute to the changes. The comparison of the radiosonde and GPS data helps validate and quantify the impact of known instrument and related changes and identify other unknown changes. In the future, the IGS products need to be better documented by incorporating details on data characteristics, how the data were derived, and more user-friendly metadata. The metadata information for radiosondes from the various sources, such as the WMO reports (WMO 2006; Gaffen 1993, 1996; Schroeder 2007), needs to be combined to create a complete global historical radiosonde metadata source.
- This study has proven how useful the GPS PW data are for monitoring the quality of global radiosonde humidity data and, in general, for climate studies because of its high accuracy, high temporal resolution, and long-term stability. In the future, every effort should be made to continue creating the IGS ZTD product and maintaining the consistency of the ZTD data in time, including minimizing changes in both instruments and analysis methods.
- As shown in this study, two observational systems are often not enough to determine which one has the problem. The WMO radiosonde intercomparison project has shown the value of more than two radiosondes on the same balloon (Nash et al. 2005). We suggest that any new observation network, such as the recently proposed Global Climate Observing System (GCOS) Reference Upper-Air Network (GRUAN; WMO 2007), should consider more than two independent and redundant observing systems for a single parameter.

Acknowledgments. This work was supported by NOAA Fund NA06OAR4310117. J. Wang would like to acknowledge the support from the NCAR Institute for Integrative and Multidisciplinary Earth Studies (TIIMES) Water Cycle Program. We thank Aiguo Dai, John Braun, Dave Parsons, and Hal Cole (all NCAR/UCAR) for constructive discussions, Joe Facundo and Bill Blackmore (both NWS) for providing the U.S. radiosonde metadata, Simon Allen and Roger Atkinson for providing the Australian radiosonde metadata, and Mary Golden (NCAR) for proofreading.

REFERENCES

Angell, J. K., W. P. Elliott, and M. E. Smith, 1984: Tropospheric humidity variations at Brownsville, Texas and Great Falls, Montana, 1958–80. *J. Climate Appl. Meteor.,* **23,** 1286–1295.

Bevis, M., S. Businger, T. A. Herring, C. Rocken, R. A. Anthes, and R. H. Ware, 1992: GPS meteorology: Remote sensing of atmospheric water vapor using the global positioning system. *J. Geophys. Res.,* **97,** 15 787–15 801.

——, ——, S. Chiswell, T. A. Herring, R. A. Anthes, C. Rocken, and R. H. Ware, 1994: GPS meteorology: Mapping zenith wet delays onto precipitable water. *J. Appl. Meteor.,* **33,** 379–386.

Bokoye, A. I., A. Royer, N. T. O'Neill, P. Cliche, L. J. B. McArthur, P. M. Teillet, G. Fedosejevs, and J.-M. Thériault, 2003: Multisensor analysis of integrated atmospheric water vapor over Canada and Alaska. *J. Geophys. Res.,* **108,** 4480, doi:10.1029/2002JD002721.

Bolton, D., 1980: The computation of equivalent potential temperature. *Mon. Wea. Rev.,* **108,** 1046–1053.

Ciesielski, P. E., R. H. Johnson, P. T. Haertel, and J. Wang, 2003: Corrected TOGA COARE sounding humidity data: Impact on diagnosed properties of convection and climate over the warm pool. *J. Climate,* **16,** 2370–2384.

Crutcher, H. L., and R. E. Eskridge, 1993: Development of a method to modify solar-induced humidity biases in the US radiosonde data from the period 1961–1973. Preprints, *Eighth Symp. on Meteorological Observations and Instrumentation,* Anaheim, CA, Amer. Meteor. Soc., 143–147.

Dai, A., J. Wang, R. H. Ware, and T. Van Hove, 2002: Diurnal variation in water vapor over North America and its implications for sampling errors in radiosonde humidity. *J. Geophys. Res.,* **107,** 4090, doi:10.1029/2001JD000642.

Deblonde, G., S. Macpherson, Y. Mireault, and P. Héroux, 2005: Evaluation of GPS precipitable water over Canada and the IGS network. *J. Appl. Meteor.,* **44,** 153–166.

Durre, I., R. S. Vose, and D. B. Wuertz, 2006: Overview of the Integrated Global Radiosonde Archive. *J. Climate,* **19,** 53–68.

Elliott, W. P., and D. J. Gaffen, 1991: On the utility of radiosonde humidity archives for climate studies. *Bull. Amer. Meteor. Soc.,* **72,** 1507–1520.

——, R. J. Ross, and B. Schwartz, 1998: Effects on climate records of changes in National Weather Service humidity processing procedures. *J. Climate,* **11,** 2424–2436.

——, ——, and W. H. Blackmore, 2002: Recent changes in NWS upper-air observations with emphasis on changes from VIZ to Vaisala radiosondes. *Bull. Amer. Meteor. Soc.,* **83,** 1003–1017.

Elms, J., 2003: Compatibility of radiosonde geopotential measurements for period from 1998 to 2001. WMO Tech. Doc. 1197, 55 pp.

Emardson, T. R., G. Elgered, and J. M. Johansson, 1998: Three months of continuous monitoring of atmospheric water vapor with a network of Global Positioning System receivers. *J. Geophys. Res.,* **103,** 1807–1820.

Fujiwara, M., M. Shiotani, F. Hasebe, H. Vomel, S. J. Oltmans, P. Ruppert, T. Horinouchi, and T. Tsuda, 2003: Performance of the Meteolabor "Snow White" chilled-mirror hygrometer in the tropical troposphere: Comparison with the Vaisala RS80 A/H-Humicap sensors. *J. Atmos. Oceanic Technol.,* **20,** 1534–1542.

Gaffen, D. J., 1993: Historical changes in radiosonde instruments and practices. WMO Tech. Doc. 541, Instruments and Observing Methods Rep. 50, 123 pp.

——, 1996: A digitized metadata set of global upper-air station histories. NOAA Tech. Memo. ERL ARL-211, 37 pp.

Gendt, G., 1998: IGS combination of tropospheric estimates—The pilot experiment. *1997 Technical Reports,* I. Mueller, K. Gowey, and R. Neilan, Eds., International GPS Services for Geodynamics, 265–269. [Available online at http://igscb.jpl.nasa.gov/overview/pubs/97techr.html.]

Guerova, G., E. Brockmann, J. Quiby, F. Schubiger, and C. Matzler, 2003: Validation of NWP mesoscale models with Swiss GPS network AGNES. *J. Appl. Meteor.,* **42,** 141–150.

Gutman, S. I., S. Sahm, S. Benjamin, and T. L. Smith, 2004: GPS water vapor observation errors. Preprints, *Eighth Symp. on Integrated Observing and Assimilation Systems for Atmosphere, Oceans, and Land Surface,* Seattle, WA, Amer. Meteor. Soc., 8.3. [Available online at http://ams.confex.com/ams/pdfpapers/72508.pdf.]

Häberli, C., 2006: Assessment, correction and impact of the dry bias in radiosonde humidity data during the MAP SOP. *Quart. J. Roy. Meteor. Soc.,* **132,** 2827–2852.

Hagemann, S., L. Bengtsson, and G. Gendt, 2003: On the determination of atmospheric water vapor from GPS measurements. *J. Geophys. Res.,* **108,** 4678, doi:10.1029/2002JD003235.

Kuo, Y.-H., W. S. Schreiner, J. Wang, D. L. Rossiter, and Y. Zhang, 2005: Comparison of GPS radio occultation soundings with radiosondes. *Geophys. Res. Lett.,* **32,** L05817, doi:10.1029/2004GL021443.

Leiterer, U., H. Dier, and T. Naebert, 1997: Improvements in radiosonde humidity profiles using RS80/RS90 radiosondes of Vaisala. *Beitr. Phys. Atmos.,* **70,** 319–336.

Li, Z., J.-P. Muller, and P. Cross, 2003: Comparison of precipitable water vapor derived from radiosonde, GPS, and moderate-resolution imaging spectroradiometer measurements. *J. Geophys. Res.,* **108,** 4651, doi:10.1029/2003JD003372.

Liou, Y.-A., Y.-T. Teng, T. Van Hove, and J. C. Liljegren, 2001: Comparison of precipitable water observations in the near tropics by GPS, microwave radiometer, and radiosondes. *J. Appl. Meteor.,* **40,** 5–15.

Lucas, C., and E. J. Zipser, 2000: Environmental variability during TOGA COARE. *J. Atmos. Sci.,* **57,** 2333–2350.

Miloshevich, L. M., H. Vömel, A. Paukkunen, A. J. Heymsfield, and S. J. Oltmans, 2001: Characterization and correction of relative humidity measurements from Vaisala RS80-A radiosondes at cold temperatures. *J. Atmos. Oceanic Technol.,* **18,** 135–155.

Nakamura, H., H. Seko, and Y. Shoji, 2004: Dry biases of humidity measurements from the Vaisala RS80-A and Meisei RS2-91 radiosondes and from ground-based GPS. *J. Meteor. Soc. Japan,* **82,** 277–299.

Nash, J., R. Smout, T. Oakley, B. Pathack, and S. Kurnosenko, 2005: WMO intercomparison of high quality radiosonde systems: Final report. WMO Rep., 118 pp. [Available online at http://www.wmo.int/pages/prog/www/IMOP/intercomparisons/RSO-2005/RSO-IC-2005_Final_Report.pdf.]

Niell, A. E., 1996: Global mapping functions for the atmosphere delay at radio wavelengths. *J. Geophys. Res.,* **101,** 3227–3246.

——, A. J. Coster, F. S. Solheim, V. B. Mendes, P. C. Toor, R. B. Langley, and C. A. Upham, 2001: Comparison of measurements of atmospheric wet delay by radiosonde, water vapor radiometer, GPS, and VLBI. *J. Atmos. Oceanic Technol.,* **18,** 830–850.

Ohtani, R., and I. Naito, 2000: Comparisons of GPS-derived precipitable water vapors with radiosonde observations in Japan. *J. Geophys. Res.,* **105,** 26 917–26 929.

Ray, J., D. Crump, and M. Chin, 2006: New GPS reference station in Brazil. *Geophysical Research Abstracts,* Vol. 8, Abstract 04919. [Available online at http://www.cosis.net/abstracts/EGU06/04919/EGU06-J-04919-1.pdf.]

Rocken, C., R. H. Ware, T. Van Hove, F. Solheim, C. Alber, J. Johnson, M. Bevis, and S. Businger, 1993: Sensing atmospheric water vapor with the global positioning system. *Geophys. Res. Lett.,* **20,** 2631–2634.

——, T. Van Hove, and R. H. Ware, 1997: Near real-time GPS sensing of atmospheric water vapor. *Geophys. Res. Lett.,* **24,** 3221–3224.

Ross, R. J., and D. J. Gaffen, 1998: Comment on "Widespread tropical atmospheric drying from 1979 to 1995" by Schroeder and McGuirk. *Geophys. Res. Lett.,* **25,** 4357–4358.

Schroeder, S. R., 2007: Using sensitive variables to validate and complete global historical radiosonde metadata—Toward computing atmospheric climate trends adjusted for instrument changes. Preprints, *14th Symp. on Meteorological Observation and Instrumentation,* San Antonio, TX, Amer. Meteor. Soc., JP1.2. [Available online at http://ams.confex.com/ams/pdfpapers/119792.pdf.]

Sharpe, M. C., and B. Macpherson, 2001: Developments in the correction of radiosonde relative humidity biases at the Met Office. Preprints, *14th Conf. on Numerical Weather Prediction,* Ft. Lauderdale, FL, Amer. Meteor. Soc., 250–253. [Available online at http://ams.confex.com/ams/pdfpapers/22640.pdf.]

Soden, B. J., and J. R. Lanzante, 1996: An assessment of satellite and radiosonde climatologies of upper-tropospheric water vapor. *J. Climate,* **9,** 1235–1250.

——, and S. R. Schroeder, 2000: Decadal variations in tropical water vapor: A comparison of observations and a model simulation. *J. Climate,* **13,** 3337–3341.

——, D. D. Turner, B. M. Lesht, and L. M. Miloshevich, 2004: An analysis of satellite, radiosonde, and lidar observations of upper tropospheric water vapor from the Atmospheric Radiation Measurement Program. *J. Geophys. Res.,* **109,** D04105, doi:10.1029/2003JD003828.

Thorne, P. W., D. E. Parker, S. F. B. Tett, P. D. Jones, M. McCarthy, H. Coleman, and P. Brohan, 2005: Revisiting radiosonde upper air temperatures from 1958 to 2002. *J. Geophys. Res.,* **110,** D18105, doi:10.1029/2004JD005753.

Tregoning, P., R. Boers, D. O'Brien, and M. Hendy, 1998: Accuracy of absolute precipitable water vapor estimates from GPS observations. *J. Geophys. Res.,* **103,** 28 701–28 710.

Turner, D. D., B. M. Lesht, S. A. Clough, J. C. Liljegren, H. E. Revercomb, and D. C. Tobin, 2003: Dry bias and variability in Vaisala RS80-H radiosondes: The ARM experience. *J. Atmos. Oceanic Technol.,* **20,** 117–132.

Van Baelen, J., J.-P. Aubagnac, and A. Dabas, 2005: Comparison of near–real time estimates of integrated water vapor derived with GPS, radiosondes, and microwave radiometer. *J. Atmos. Oceanic Technol.,* **22,** 201–210.

Vömel, H., and Coauthors, 2007: Radiation dry bias of the Vaisala RS92 humidity sensor. *J. Atmos. Oceanic Technol.,* **24,** 953–963.

Wade, C. G., 1994: An evaluation of problems affecting the measurement of low relative humidity on the United States radiosonde. *J. Atmos. Oceanic Technol.,* **11,** 687–700.

——, and B. Schwartz, 1993: Radiosonde humidity observations near saturation. Preprints, *Eighth Symp. on Meteorological Observations and Instrumentation,* Anaheim, CA, Amer. Meteor. Soc., 44–49.

Wang, J., 2002: Understanding and correcting humidity measurement errors from Vaisala RS80 and VIZ radiosondes. *Proc. Radiosonde Workshop,* Hampton University, VA, 7 pp. [Available online at http://www.eol.ucar.edu/homes/junhong/paper/RadiosondeWS02.pdf.]

——, and K. Young, 2005: Comparisons of 7-year radiosonde data from two neighboring stations and estimation of random error variances for four types of radiosondes. Preprints, *13th Symp. on Meteorological Observations and Instrumentation,* Savannah, GA, Amer. Meteor. Soc., 3.5. [Available online at http://ams.confex.com/ams/pdfpapers/94104.pdf.]

——, H. L. Cole, and D. J. Carlson, 2001: Water vapor variability in the tropical western Pacific from a 20-year radiosonde data. *Adv. Atmos. Sci.,* **18,** 752–766.

——, ——, ——, E. R. Miller, K. Beierle, A. Paukkunen, and T. K. Laine, 2002a: Corrections of humidity measurement errors from the Vaisala RS80 radiosonde—Application to TOGA COARE data. *J. Atmos. Oceanic Technol.,* **19,** 981–1002.

——, A. Dai, D. J. Carlson, R. H. Ware, and J. C. Liljegren, 2002b: Diurnal variation in water vapor and liquid water profiles from a new microwave radiometer profiler. Preprints, *Sixth Symp. on Integrated Observing Systems,* Orlando, FL, Amer. Meteor. Soc., 198–201.

——, D. J. Carlson, D. B. Parsons, T. F. Hock, D. Lauritsen, H. L. Cole, K. Beierle, and N. Chamberlain, 2003: Performance of operational radiosonde humidity sensors in direct comparison with a chilled mirror dew-point hygrometer and its climate implication. *Geophys. Res. Lett.,* **30,** 1860, doi:10.1029/2003GL016985.

——, L. Zhang, and A. Dai, 2006: A global, 2-hourly atmospheric precipitable water dataset from IGS ground-based GPS measurements: Scientific applications and future needs. *Proc. Int. GNSS Service (IGS) Workshop 2006,* Darmstadt, Germany, European Space Agency, 1–12.

——, L. Zhang, A. Dai, T. Van Hove, and J. Van Baelen, 2007: A near-global, 8-year, 2-hourly data set of atmospheric precipitable water from ground-based GPS measurements. *J. Geophys. Res.,* **112,** D11107, doi:10.1029/2006JD007529.

WMO, 2006: Observing stations and WMO catalogue of radiosondes. WMO Publ. 9, Vol. A. [Available online at http://www.wmo.ch/pages/prog/www/ois/volume-a/vola-home.htm.]

——, 2007: GCOS Reference Upper Air Network (GRUAN): Justification, requirements, siting, and instrumentation options. WMO Tech. Doc. 1379, 42 pp. [Available online at http://www.wmo.ch/pages/prog/gcos/Publications/gcos-112.pdf.]

Zipser, E. J., and R. H. Johnson, 1998: Systematic errors in radiosonde humidities: A global problem? Preprints, *10th Symp. on Meteorological Observations and Instrumentation,* Phoenix, AZ, Amer. Meteor. Soc., 72–73.

Zurbenko, I., P. S. Porter, S. T. Rao, J. Y. Ku, R. Gui, and R. E. Eskridge, 1996: Detecting discontinuities in time series of upper-air data: Development and demonstration of an adaptive filter technique. *J. Climate,* **9,** 3548–3560.